



저작자표시-비영리-변경금지 2.0 대한민국

이용자는 아래의 조건을 따르는 경우에 한하여 자유롭게

- 이 저작물을 복제, 배포, 전송, 전시, 공연 및 방송할 수 있습니다.

다음과 같은 조건을 따라야 합니다:



저작자표시. 귀하는 원저작자를 표시하여야 합니다.



비영리. 귀하는 이 저작물을 영리 목적으로 이용할 수 없습니다.



변경금지. 귀하는 이 저작물을 개작, 변형 또는 가공할 수 없습니다.

- 귀하는, 이 저작물의 재이용이나 배포의 경우, 이 저작물에 적용된 이용허락조건을 명확하게 나타내어야 합니다.
- 저작권자로부터 별도의 허가를 받으면 이러한 조건들은 적용되지 않습니다.

저작권법에 따른 이용자의 권리는 위의 내용에 의하여 영향을 받지 않습니다.

이것은 [이용허락규약\(Legal Code\)](#)을 이해하기 쉽게 요약한 것입니다.

[Disclaimer](#)

**A THESIS
FOR THE DEGREE OF DOCTOR OF PHILOSOPHY**

**Sensor-embedded Kidney and Liver
Microphysiological Systems for Drug and
Disease Analysis**

Arun Asif

**DEPARTMENT OF MECHATRONICS ENGINEERING
GRADUATE SCHOOL
JEJU NATIONAL UNIVERSITY
REPUBLIC OF KOREA**

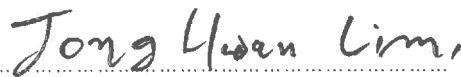
February 2022

Sensor-embedded Kidney and Liver Microphysiological Systems for Drug and Disease Analysis

Arun Asif
(Supervised by Professor Dr. Kyung Hyun Choi)

A thesis submitted in partial fulfillment of the requirements for the degree of
Doctor of Philosophy
February 2022

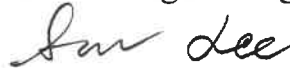
This thesis has been examined and approved.



Thesis Committee Chair, **Prof. Jong Hwan Lim**,
Mechatronics Engineering Department



Thesis Committee Vice-Chair, **Prof. Chul Ung Kang**,
Mechatronics Engineering Department



Thesis Committee Member, **Prof. Sun Ryung Lee**,
Biology Department



Thesis Committee Member, **Prof. Sang Ho Lee**,
Pharmacy Department



Thesis Director, **Prof. Kyung Hyun Choi**,
Mechatronics Engineering Department

DEPARTMENT OF MECHATRONICS ENGINEERING
GRADUATE SCHOOL
JEJU NATIONAL UNIVERSITY

Preamble

This thesis is submitted for partial fulfillment of the requirements for the degree of Doctor of Philosophy in Department of Mechatronics Engineering at Jeju National University, Republic of South. All the research work presented here, was established in Advanced Micro-Mechatronics Lab at Jeju National University. No content or segment of this thesis has been submitted for any degree at any other institution or university. This thesis work is original according to the best of author's knowledge unless reference is taken from relating work published. Content from this thesis has already been published in 2 research articles in international peer reviewed journals listed below.

1. **Asif, A.**, Park, S.H., Manzoor, A., Khalid, M.A.U., Salih, A.R.C., Kang, B., Ahmed, F., Kim, K.H. and Choi, K.H., 2021. Microphysiological System with Continuous Analysis of Albumin for Hepatotoxicity Modeling and Drug Screening. *Journal of Industrial and Engineering Chemistry*. 98, pp.318-326.
2. **Asif, A.**, Kim, K.H., Jabbar, F., Kim, S. and Choi, K.H., 2020. Real-time sensors for live monitoring of disease and drug analysis in microfluidic model of proximal tubule. *Microfluidics and Nanofluidics*, 24, pp.1-10.

My thesis is dedicated to my parents who have sacrificed a lot giving me what they couldn't have in their lives, and they backed my decision of going to South Korea for PhD degree in spite of other available options and Dr. Afaque Manzoor Soomro for helping me in every step of my PhD.

ACKNOWLEDGMENT

Looking back when I was in high school, I never thought of doing PhD but here I am completing my PhD degree from Jeju National University. I strongly believe that all the academic and social success in my life is because of the blessings and efforts of my parents. Since my childhood, I was continuously supported, taught, encouraged, and inspired by my mother, Dilshad Akhtar, and my father, Asif Ernest Gill, and my late grandparents William John Gill and Treasa William. My parents have sacrificed a lot.

Before going to South Korea, I had so much self-doubt about everything, yet I was hopeful for a better tomorrow, and it happened to be a better time in my life. Things were not as smooth as I expected. I got to face numerous hardships be it social, emotional, physical, or laboratory environment. Overall, I came out stronger and fierce for tackling future problems. I am thankful and hopeful that this PhD degree has given a positive direction to my career. I want to give credit to myself for never giving up on myself in this PhD. It was possible because of my senior, my mentor, and a sincere friend Dr. Afaque Manzoor Soomro who supported and encouraged me at every setback and made me realize my value as a human, as a friend, and as a researcher.

Family and friends play a great role in one's life and I am thankful that I have been bless with amazing people as my family and friends who were always there to listen to me. My parents and my siblings have been a great support and source of motivation throughout my life. I thank my older sister, Anum, and younger brother, Zaroon, for always having my back and being my source of happiness and courage.

I want to thank my teachers who have helped me in building such an attitude of perseverance and being patient. First of all, I thank Professor Dr. Kyung Hyun Choi,

my PhD supervision, who guided me in earning this PhD Degree. Professor Choi trusted my research ideas that later became research publication in well reputed journals. Then, I want to thank my MS supervisor, Dr. Sobia Manzoor who has been a great mentor from the start of my research career. Her support, encouragement and guidance has given me a confidence in science and humanity. I mainly learnt the true essence of being a scientific researcher from Dr. Sobia and I am deeply thankful for that.

Overall, I feel satisfied with my life. I have had a lot of experiences, either good or bad, but those experiences made me what I am today that is better than my past self. I enjoyed a lot of adventurous things in South Korea, I met amazing people. At times, I faced several rejections, especially in research paper publication process, but I kept myself hopeful with the thought that “rejection leads to perfection.”

Spiritually, I am so much overwhelmed and thankful to Jesus Christ for showing so many miracles in my life. As they say that, “the best lesson is hard learned and the best reward is hard earned” and it’s the journey that counts, not the destination. I feel proud that I happened to come to Korea for my PhD to develop my profile. It was the will of God that brought me here to accomplish so much which I never thought of. Lastly, I would thank all my lab fellows, seniors, juniors for their best wishes.

Arun Asif

November 29, 2021

Table of Contents

Table of Figures	VII
Abstract.....	IX
1. Objectives of Thesis.....	1
2. Introduction.....	2
3. Research Background	5
3.1. Kidney Microphysiological System	5
3.2. Liver Microphysiological System	6
3.3. Microfluidic Sensors	8
3.3.1. Electrochemical Sensor.....	8
3.3.2. Impedimetric Sensor	9
3.3.4. Electrochemical Immunosensor.....	10
4. Methodology	12
4.1. OoC-based MPS Design and Development	12
4.2. Sensor Development	13
4.2.1. Transepithelial Electrochemical Resistance Sensor.....	13
4.2.2. Albumin Immunosensor Development for Liver MPS.....	14
4.3. OoC Models	17
4.3.1. Kidney MPS Cell Culture	17
4.3.2. Liver MPS Cell culture	17
4.4. Biochemical Assays	18
4.4.1. Viability Assay and ELISA Measurement from Kidney MPS	18
4.4.2. Albumin, Urea, and P450 Assays	19
4.4.3. Immuno-fluorescence Staining	19
4.5. Computational Fluid Simulation	20
4.6. Statistical Analysis	20
5. Results.....	21

5.1.	Kidney MPS with TEER Sensor	21
5.1.1.	Proximal Tubule Cells and Fibroblasts Mixed Culture	21
5.1.2.	Inflammatory Nephrotoxicity	21
5.1.3.	Drug Treatment.....	22
5.1.4.	Viability Analysis	25
5.1.5.	KIM-1 and HSP70 ELISA Measurements.....	26
5.2.	Liver MPS with Albumin Immunosensor	27
5.2.1.	Electrochemical Analysis of Human Serum Albumin Sensor.....	27
5.2.2.	Liver MPS Design.....	27
5.2.3.	Sensor Testing for 24 Hours	28
5.2.4.	Sensor Testing for 6 Days.....	29
5.2.5.	Biochemical Measurements	31
5.2.6.	Fluid Dynamics Simulation	32
6.	Discussion	34
7.	Conclusion and Future Perspectives	36
	References.....	37

Table of Figures

Figure 1. (a) Proximal Tubulopathy. Cellular damage triggered due to hyperglycemic conditions. (b) Schematics of the proximal tubule on a chip model.....	6
Figure 2. Schematics of liver MPS of liver-on-a-chip with albumin immunosensor.	8
Figure 3. Schematics of MPS experiment, inset shows the zoomed chip setup and microfluidic channel design.....	13
Figure 4. a) Chip schematic and electrode dimensions. b) Surface modifications pattern with immobilization of antibody. c) electrodes in chip assembly with microfluidic channels. d) 50X magnification microscopic picture of electrodes.	15
Figure 5. Relative Result of TEER sensor in multiple conditions. (a). Impedance graph for cells after treatment of normal media. (b). Impedance graph for cells after treatment of glucose containing media. (c). Impedance graph for cells after treatment of drug containing media. (d). pH measurement for relative pH trend in normal media, high glucose media and drug-containing media for 5 days. (e). Live-Dead Assay results for cells under normal media, high glucose media and drug-containing media. F. ELISA results for protein biomarkers.	23
Figure 6. Light microscopy pictures of fibroblast and HK-2 cells. (a) Normal media represented good confluent monolayer of cells. (b) Microscopic Images from platform integrated microscope with an interval of five days of incubation with normal media, high glucose media and drug-containing media (scale bar is 100 μ m, and pictures are captured at 100X).....	24
Figure 7. Representative pictures of cell viability assay using confocal microscopy. .	25
Figure 8 ELISA result of KIM-1 and HSP70 proteins. In each experimental phase, media was stored from 3rd and 5th day i.e., normal media, high glucose, and drug media. Concentrations shown in mean \pm S.E.M.....	26
Figure 9. Sensor Characterization a) plot showing the stability of the sensor because of CV test b) Plot showing the testing results for confirming the Rct of the sensor c) Plot showing the relation between frequency and impedance. d) Curve at given frequency of 18.078 Hz for calibrating the sensor.....	27
Figure 10. Immunosensor Measurements. a) Specific albumin concentrations at specific time-points in 24-hour experiment. b) Total albumin concentrations at specific time-points in 24-hour experiment. c) Specific albumin concentrations at specific time-points	

in 6- day experiment. d) Total albumin concentrations at specific time-points in 6-day experiment.....	30
Figure 11. A comparison of albumin concentration measurements taken by immunosensor versus ELISA kit. a) 24-hour experiment result. b) 6-day experiment result.....	30
Figure 12. Molecular biomarker results, Chip denotes Liver MPS and 2D denotes petri dish a) comparison of albumin secretion between 3D and 2D culture. b) comparison of urea excretion between 3D and 2D culture. c) comparison of P450 activity between 3D and 2D culture.....	32
Figure 13. Fluorescence Microscopy for albumin staining at termination of 6 days long experiment. Microscopy results are aligned with other molecular assay and sensor analysis further affirming the development of disease and recovery model.	32
Figure 14. Simulation results of computational fluid flow analysis in the microfluidic channel (pressure scale shown on left).	33

Abstract

Advanced cell culture technique, organ-on-a-chip (OoC) caters the capacity to mimic human physiology with reverse engineered biological formulation of human organs and multi-organs. The prime perspective of 3D cell culture is engineering human physiology for disease modeling to enhance drug screening analytics. Mimicking human physiology with complex *in vitro* model brings the prospect to replace the usage of laboratory animals for drug screening. Human metabolism is primarily carried out in liver with its excretion taking place in kidney makes these two organs vital for drug screen studies. Additionally, current OoC based MPS systems are mainly dependent upon conventional end-point bioassays comprising of PCR, western blots, and biochemical assays. It is challenging to perform conventional bioassays to analysis MPS systems owing to their complexity as well as reduced cell number and culture media quantity for sample collection. Such analytical limitation in MPS highlights the potential to integration the real-time or continuous sensors for efficient monitoring of cell conditions and responses. This thesis work encompasses the development of microfluidic liver and kidney MPS systems to emulate the development of disease and drug treatment with the integration of sensors. Liver and Kidney MPS were established with the integration of impedance-based transepithelial electrochemical resistance (TEER) sensor, optical pH sensor, and albumin immunosensor for monitoring of disease model development and drug efficacy measurements which were further validated by conventional bioassays. As albumin exhibits the function, the integrated microfluidic human serum albumin immunosensor facilitated the albumin screening for disease and drug analysis. This thesis contributes for the improvement of continuous monitoring of MPS by expanding the disease modeling capacity of OoC technology for a rapid development of drugs.

1. Objectives of Thesis

The main objectives in the current thesis focus on the design of a liver MPS and proximal tubule MPS in a microfluidic chip with capacity to imitate cytotoxic effect of high glucose in the microenvironment of liver and proximal tubule, respectively, with embedded sensors. Current MPS facilitate continuous measurements of TEER and human serum albumin. Transparent electrode system was printed using indium tin oxide (ITO) for TEER measurements which facilitated image capturing during the experiment. Functionalized gold-based electrode system was developed in a microfluidic manner then linked with liver MPS model for long-term continuous albumin measurement. Diabetic hepatopathy and diabetic nephropathy models were established using high glucose media for a certain period of time and anti-diabetic drug was administered for examining the recovery of the MPS. The embedded sensors presented a sound analysis of the disease development and tissue recovery after drug treatment which was validated using the molecular assays data. The developed platforms may provide with an efficient method to analyze the toxicity and efficacy of drugs in different disease models at a faster pace and reduced cost as compared to animal models. The MPS platforms will be crucial for the earlier ADME-Tox i.e., absorption, distribution, metabolism, excretion and toxicity, data of drugs for better understanding of their pharmacokinetics.

2. Introduction

There is a dire need to mimic the complexity of human tissues and organs in laboratory to better understand human physiology for disease and drug analysis. Historically, scientific cell culture started in late 19th century and “Petri dish” was adopted as a standard vessel for two dimensional (2D) cell culture (1, 2). Recently, cell culture techniques are evolving into advanced three-dimensional (3D) culture tools to mimic human tissues, organs and organ functions at micro and nanoscale (3-5). Cancer and viral diseases remain a big challenge for the mankind to overcome which can be possible by improving the capacity to mimic human physiology in the best possible way (6-9). This microscale mimicry of human physiology is executed in microphysiological systems (MPS). The development and design principle of MPS is dictated by the end goals of the study purpose and target tissue or organs. The devices for making 3D cell culture-based MPS have transformed cells into Transwell TM, Organ-on-a-Chip (OoC), spheroids plates, organoids dishes or chips, air-liquid interphase methods, microfluidic culture systems, and cell sheets for demonstrating multiple microphysiological applications to fulfill multiple contexts of use (10).

Among latest 3D cell culture techniques, OoC has become of the top methods to mimic human physiology at microlevel. The biggest challenge posed to drug development is the irrelevant pathophysiological outcomes in humans with correlation to 2D cell culture and animals (11). OoC development began with the idea to replace the animal models with an alternative system to mimic human specific cells, organs, functions, organization, and their cross-communication in the most relevant method if not exactly (12, 13). The exact emulation of human biology is required to have higher success rate for drug discovery and development subsequently reducing the time and cost for more effective remedies (14, 15). OoCs have successfully been establishing a

broader range to imitate human physiology with reverse engineered biological formulation of human organs. Understanding the cellular conditions and responses to multiple external cues which were not possible in 2D culture or animal models, are facilitating for better *in vitro* studies. Engineering human physiology for disease modeling to improve drug screening analytics is the primary goal of 3D cell culture. The use of complicated *in vitro* models to mimic human physiology has the potential to eliminate the use of laboratory animals for drug testing. As human metabolism is predominantly carried out in the liver and excretion occurs in the kidney, these two organs are critical for drug screening studies.

Liver is the primary hub of metabolism for all foreign particles entering into the human body and detoxifies them for excretion. Hence, liver plays a pivotal role in drug biotransformation and immune response to infectious particles. Liver consists of 4 major cell types i.e., hepatocytes, stellate cells, Kupffer cell (liver macrophage), and liver sinusoidal endothelial cell (LSEC), which are necessary to maintain its physiology, metabolic capacity, and immunological response. The above given qualities of liver are required in an MPS to mimic the disease and drug toxicity depending on context of use. Likewise, kidney performs filtration, reabsorption, and fluid excretion to maintain fluid homeostasis in body. Emulation of kidney function in a microfluidic device may facilitate the pre-clinical drug testing in regard to predict drug induced nephrotoxicity.

Moreover, traditional end-point bioassays such as PCR, western blots, and biochemical tests are heavily used in modern OoC-based MPS systems. Because of their intricacy, as well as the limited number of cells and culture media available for sample collection, performing traditional bioassays to analyze MPS systems is difficult. The possibility for integrating real-time or continuous sensors for efficient monitoring of cell conditions and responses is highlighted by such analytical limitations in MPS.

Microfluidic biosensors present a great potential to be attached with MPS for continuous monitoring of the microscale changes occurring in tissue microenvironment. Biosensors are defined as tools with the capacity to recognize signal generated from target analyte i.e., tissue, cells, proteins, DNA, RNA, sugars, or fat molecules, through the attached transducer both qualitatively and/or quantitatively. Transepithelial electrochemical resistance (TEER) sensor presents potential to measure the tissue formation in the microfluidic culture chamber based on impedance change in response to cell growth. Immunosensor measure the concentration of the analyte present in the fluid based on the electrochemical (impedance) change resultant to antigen-antibody attachment on the electrodes. The integration of TEER sensor and immunosensor enhance the analytic potential of microfluidic MPS for continuous data collection regarding multiple drugs ultimately speed-boosting the drug development process.

The creation of microfluidic liver and kidney MPS systems for disease and therapeutic research with the incorporation of sensors is the focus of this thesis. The integration of an impedance-based transepithelial electrochemical resistance (TEER) sensor, an optical pH sensor, and an albumin immunosensor was used to monitor disease model development and drug efficacy assessments, which were then confirmed using standard bioassays. The integrated microfluidic human serum albumin immunosensor enabled albumin screening for disease and medication analysis because albumin has the function. By improving the disease modeling capacity of OoC technology for rapid drug development, this thesis contributes to the improvement of continuous monitoring of MPS.

3. Research Background

3.1. Kidney Microphysiological System

Newly evolving OoCs based bio-microfluidic tools carry the capacity to transform testing of drugs by decreasing, if not substituting, the use of animals for drug development. Field of OoCs is progressing since the earlier efforts of cell culturing within microfluidic environment up to progression towards multiorgan models on a chip for developing better MPS (16). As of biological viewpoint, OoC technology is growing into advance culture techniques such as organoid and spheroid culture on chips (17). Lately, pharma industry observed a significant drop in investigation and innovation efficiency owing to the surge in drug failure percentage at clinical stages (18). Typically, the success percentage for the development of drugs is reduced to below 12% of all proposed drugs in the past 10 years leading to massive economic losses for pharmaceuticals (19). The drug discovery and development cost for a single drug till the time of its FDA approval has surged up to more than 2 billion US dollars due to increase failure of potential drug targets (20). The field of OoCs prospects the strategic goals for the elimination of ineffective lead candidates in the most early feasible stages to lower the economic burden and time constraints.

The prevalent chronic diseases including, obesity, hypertension, and diabetes, promote strains and damage on kidney(21). Overtime, kidney functions are declined because of diabetic conditions (22). Constant state of albuminuria in blood develops cell injury initiating tubulopathy which leads to the progression of inflammation in proximal tubule as shown in Fig. 1a (23).

Shear stress plays crucial role and stimulates modifications in tissue both structurally and functionally because of various mechanical and sensory processes not possible in traditional 2D cell culturing technique (24). Cellular attachment capacity

and response to external factors are also affected by shear stress (25). To model nephrotoxicity, OoC technology presents an appropriate environment to simulate kidneys to screen potential drugs, still there is a need of continuous analysis of OoC technology (16).

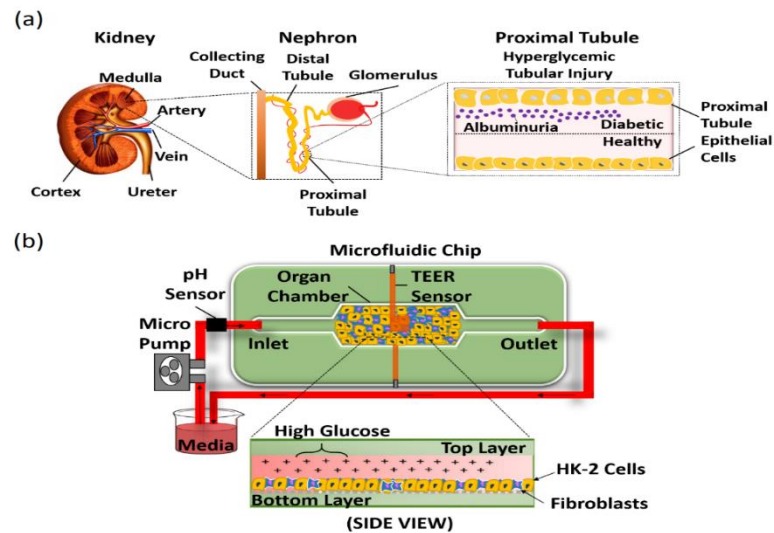


Figure 1. (a) Proximal Tubulopathy. Cellular damage triggered due to hyperglycemic conditions. (b) Schematics of the proximal tubule on a chip model.

3.2. Liver Microphysiological System

Liver performs essential function to metabolize drugs (26). Microphysiological model systems for liver have come up as an effective instruments for testing of drugs because of their ability to imitate humans' pathophysiology (27). As of a limited applicability and irrelevancy of toxicity predictions for drugs being tested in animals for their potential use in human disease treatment, the recent emergence of various *in vitro* liver model systems primary, MPS like liver-chips, are replacing animal models for predicting clinical outcomes of the drugs (28, 29). Previous developments in *in vitro* hepatic microphysiological model systems mainly consist of, hepatics organoid models (30, 31), hepatic tissues made from 3D-printing (32, 33), and liver-on-a-chip (34-37).

To analyze the functionality of liver, human serum albumin (HAS) has come up as an important marker for indicating the liver condition. HAS is steadily released from main unit of liver cell, hepatocyte (38). The change in the concentration of albumin in human serum can be directly correlated with the health and disease condition of liver as well as the effect of a drug can be analyzed using albumin as an efficacy biomarker (39). Albumin is present in human's plasma as a biomolecule with the highest concentration and plays a vital function in the homeostasis of body fluids (40, 41). Multiple functions such as, balance of vitamins and toxins, sustaining fatty acids, balance of hormones, and maintenance of drug transport are facilitated with the presence of HSA in the blood (42, 43). All the aforementioned characteristics of HSA presents itself as one of the most important and a clinically significant biomarkers owing to its impact in the pathogenesis of hypo- and hyper-albuminemia (44).

Latest trends in the biosensor development have shown their potential in microfluidics which further presents their capacity to be attached with MPS to monitor the cellular conditions (45-47). In comparison with traditional manual and exhaustive procedures including, western blotting and ELISA, the sensors based upon microfluidics to analyze biomarkers may contribute greatly for the measurements while dealing with limited volume of sample (48-50). Currently, it is the need of the hour to find an alternative approach to animal models for the toxicity testing of drugs. Similar

to diabetic nephropathy, a model is required to mimic diabetic liver pathogenesis to have speed-boost the development of drugs for diabetic patients.

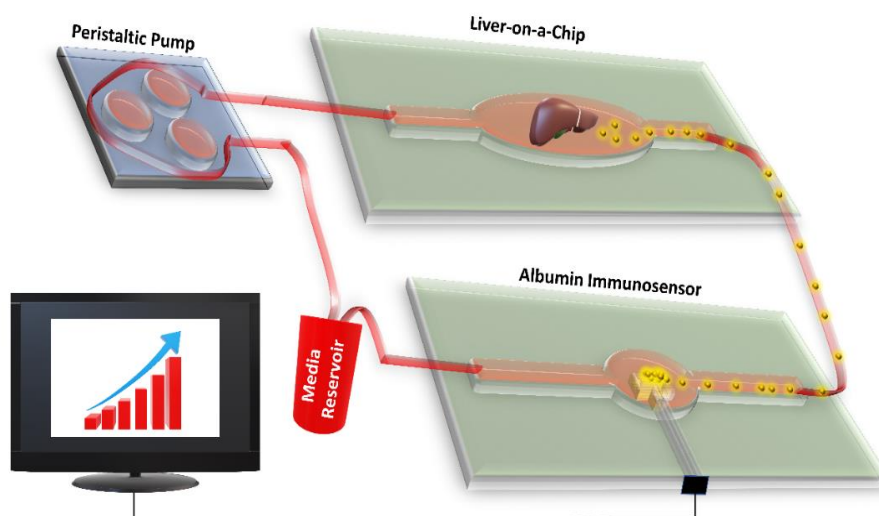


Figure 2. Schematics of liver MPS of liver-on-a-chip with albumin immunosensor.

3.3. Microfluidic Sensors

3.3.1. Electrochemical Sensor

An electro-chemical sensor is defined as a device which provides with the electrical signal information caused by chemical reaction in a system composition instantly by combining a chemically selective layer (electrodes – charge recognizing elements) to an electro-chemical detector also known as “transducer”. In simple words, an electrical energy produced due to a chemical reaction is transformed into analytical signal which are detected by transducer (51). Electrochemical sensor belongs to the oldest category of chemical sensors owing to their simple development process, ease of miniaturization and the capacity to be integrated with system without a compromise in the detection and analysis (52).

Electrochemical sensors are distributed into multiple categories owing to their recognition capacity of transduction depending on electric magnitude i.e., amperometric or voltametric, impedimetric, conductometric, and potentiometric. The concept design of a chemical sensor depends on the specific recognition of the analyte – the molecule of interest. Highly specific element is selected for the development of a specific sensor for specific recognition.

Main characteristics in a sensor design comprise of; immediate response, improved chemical stability, higher mechanical sustainability (53). Several biosensors overcome the mechanical and chemical limitations by using highly selective biological molecules for analyte recognition. The attachment of receptor molecules is also known as molecularly imprinted polymers which artificially work as a sensor being attached to an electrode (54). The use of biological receptors in sensor development is in its initial stages due to the challenges such as the laborious process of development and intrinsic biochemical principles of attachment.

3.3.2. Impedimetric Sensor

Impedance measurement sensor system is usually nonselective which is made selective by fixing a recognition element in the system, e.g., biochemical molecules, which transform it to a selective method. In impedimetric sensor, measurement is made using alternating current (AC) among two electrode system (working and counter) with a reference electrode in response to which an AC voltage is generated for the measurement. As only a negligible current pass through the reference electrode, the impedimetric sensor can be made function only by using 2 electrode system. Overall, the impedance can be defined as AC resistance.

A phase difference among response current and voltage is generated in case of application of sinusoidal voltage leading to resistive and capacitive impedance against the flow of current. Impedance is represented by “Z” as follows.

$$Z = R + j X_C$$

The real dimensions and imaginary parts present the phase delay components of 0 degree and 90 degrees respectively. R “resistive factor” shows a critical dependence on electrical conductance defects of an electrochemical cell. Principally, the changes in conductance are in reciprocal values to resistance which is generated by the change in mobility, ions, or charge, in an electrochemical cell. Conversely, the resistance in capacitance represented by X_C , is produced by the charge in the double layered electrode surface. In case of dominance by the capacitance, the sensor is represented by as capacitive. The dielectric property of electrical insulating layer is defined as capacitance. Capacitance comprises of recognition element and the conductive phases of electrolyte and electrode. The change in the dielectric constant is measured as impedance change.

3.3.3. Transepithelial Electrochemical Resistance (TEER) Sensor

TEER is monitored to measure the impedance change across the cellular barrier in an electrode system. Mainly tight-junction proteins are kept as the reference molecules to measure the barrier function in a tissue. TEER sensor performs the paracellular permeability of voltage in two electrodes across the cell monolayer (55). The previous models of TEER sensors include examples as, an assembly of electrodes on glass layer embedded in culturing vessel (56), cell culture chamber accompanied with two large electrode system (57), or a system of wires embedded above and below the cellular layer (58). Despite the effective attempts to combine the gold-based electrode assembly with multielectrode arrays in cell culture chambers the opportunity to take images has been compromised due to opaque nature of electrodes. A transparent TEER sensor may provide with the opportunity to capture images of cell monolayer without interference of the electrodes.

3.3.4. Electrochemical Immunosensor

An electrochemical immunosensor consists of three main components including, recognition element (bioreceptor i.e., enzymes, antibodies, cell, etc.), a transducer and the electronic system. The specific identification of target analytes is performed by the biorecognition element making it the fundamental part of biosensors. Immunosensor work on the principle of antibody and antigen attachment. Antibody is an immunoglobulin molecule which recognizes the antigen (target analyte). Antigen and antibody show a strong natural affinity and specificity.

Electrochemical immunosensor technology is proving to be a highly selective and efficient tool for the target analyte detection. The immune reaction is conveniently combined with the transducer making them a powerful tool for analyte analysis. The incidence of analyte attachment at the electrode surface creates a potential in the double

layer, making the electron flow (potential) in a direct proportion to the concentration of antigen. In general, the functionality of an immunosensor is derived by immobilizing antibody on the electrode surface and later the antigen is added to the system for monitoring.

Electrochemical immunosensor analysis is usually performed using electrochemical impedance spectroscopy (EIS) method to measure the interphase change difference in the impedance. EIS provides with a lesser electrical interference with steady and reproducible response. Immunoreaction produces variance in the charge transfer resistance represented as “ R_{ct} ”, which follows Randle’s equivalent circuit model. Several nanomaterial composite types have been employed to increase immunosensor performance such as nanoparticles, magnetic beads, carbon nanotubes, and graphene oxide. Multiple methods can be used to immobilize the capturing antibody such as, electrostatic entrapment, physical adsorption, or covalent attachment. Immunosensors present a great deal of diagnostic application in future owing to their reproducibility, stability, and reliability.

Formerly created microfluidic immunosensors to detect human serum albumin were particular to a specific system or had a limited duration ability for extended time-period analysis of cell response to drugs and stimulants (47). Liver MPS interconnected to continuous monitoring in response to biomarkers could be reliable in toxicity analysis of new drugs. Moreover, innovations in the design of liver-chips from earlier versions to various goals for mimicking hepato-physiology yet, the models for emulation of liver in diabetic condition to monitor the continuous impact of drug for diabetic patients.

4. Methodology

4.1. Organ Chip-based MPS Design and Development

A microfluidic chip using glass layers was assembled with 2 1.1 mm thick soda-lime pieces of glass consisting of dimensions having 41 mm width and 56 mm length. Microchannel was created with the printing of silicon elastomers (Musil MED-6033) with dimensions having 200 μm height (h) and 900 μm width by an in-house built 3D inkjet printer. Microchannel width was kept 3 mm and the width of chamber for cell culture consisted of 9 mm with a length of 20 mm giving an area of 180 mm^2 for cell culturing

The media circulation was made possible using peristaltic pump connecting the media reservoir with microfluidic chip. The mimic the tissue microenvironment presents in tubular section of nephron, a similar shear stress was provided by giving similar fluid flow conditions in the microfluidic chip. A complete microfluidic MPS setup is displayed in Fig. 3.

Previously, described flow-based shear-stress value in proximal tubular section of nephron is 5 Dyne/ cm^2 (59). To provide 5 dynes/ cm^2 of shear stress value to proximal tubular monolayer, flow of media was adjusted on 60 $\mu\text{l}/\text{min}$. Shear stress caused by media in microfluidic channels can be determined using the reference (60);

$$\tau = \frac{6\mu Q}{wh^2}$$

τ represents shear stress (5 dynes/ cm^2), rate of media flow is represented with “Q” 60 $\mu\text{l}/\text{min}$, whereas “ μ ” is representing the value of fluid viscosity (0.8 $\text{mPa}\cdot\text{s}$) which is being flowed in channel. The channel width is represented by “w” (900 μm) and the channel height is shown as “h” (200 μm).

Like kidney MPS, in liver MPS the flow rate calibration was done for emulating shear-stress in liver epithelia. The value of shear stress present in liver epithelia is determined at ~ 5 dynes/cm² and it was calculated according to the above given equation

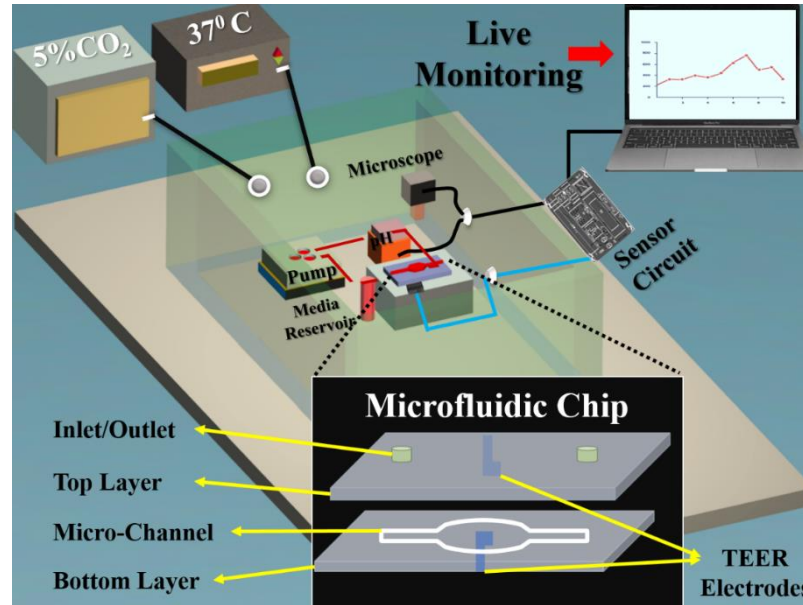


Figure 3. Schematics of MPS experiment, inset shows the zoomed chip setup and microfluidic channel design.

4.2. Sensor Development

4.2.1. Transepithelial Electrochemical Resistance Sensor

Square-shaped ITO electrode was fabricated on each glass in the middle of cell culturing space on the chip for the establishment of TEER sensor. The dimension of the electrode consisted of 500 normal media in thickness 4 mm in length. A screen printing method was used to print the ITO electrodes on the glass chip. One The area of one ITO electrode kept at 16 mm². LabVIEW platform was employed to develop a software for the measurement of change in impedance values. Impedance values were recorded in Ohm millimeter square (Ω mm²).

Each glass layer was assembled in a chip-holder in such a way that each ITO electrode was positioned to be opposite to each other and a circuit for electrical

resistance measurement was completed. A calibration process was followed to decide the best suitable frequency for TEER measurements. A frequency showing the maximum impedance against the development of cell monolayer was selected to be used for taking impedance values at. A range of frequency consisting of 1 to 10000 was selected for impedance change. Arduino microcontroller was used for the calibration of impedance which provided a sinusoidal voltage of 0.1 V. A final frequency of 58.7 Hz was optimized to continuously monitor impedance change during the development of cell monolayer (5).

4.2.2. Albumin Immunosensor Development for Liver MPS

For liver MPS, the similar design to kidney MPS was used but without a TEER sensor and for the development of albumin immunosensor, a similar chip was taken with printed electrodes at the middle of cell culture chamber containing a working electrode, counter electrode, and reference electrode (8). The electrode pattern was fabricated by a multi-head system based on Electrohydrodynamic (EHD) for ink-jet printing (Fig.4). Gold-ink (Au) was used to print working and counter electrodes while silver-ink was utilized for the printing of reference.

a. Surface Modification

To immobilize antibodies on the gold electrode, there need to be a thiol-based self-assembled monolayer to facilitate the attachment. First of all, the gold electrode is properly cleaned and then, MPA solution in ethanol (3-Mercaptopropionic acid, Sigma®) is applied for the formation of thiol bonds. Later, functionalized electrodes are rinsed with DI water. Then for the development of self-assembled monolayer, a 1:1 mixture of NHS and EDC solution, N-Hydroxysuccinimide (NHS) (130672, Sigma-Aldrich®, Seoul, South Korea) and 1-ethyl-3-(3-dimethylaminopropyl) carbodiimide hydrochloride (EDC) (03449, Sigma-Aldrich®, Seoul, South Korea) was treated. Later,

excess EDC/NHS was removed for subsequent immobilization of albumin antibody “ab2406, Abcam”. In the last step, 1% BSA was treated for blocking unbound sites on the electrodes and Fig. 4 shows the electrode pattern on chip.

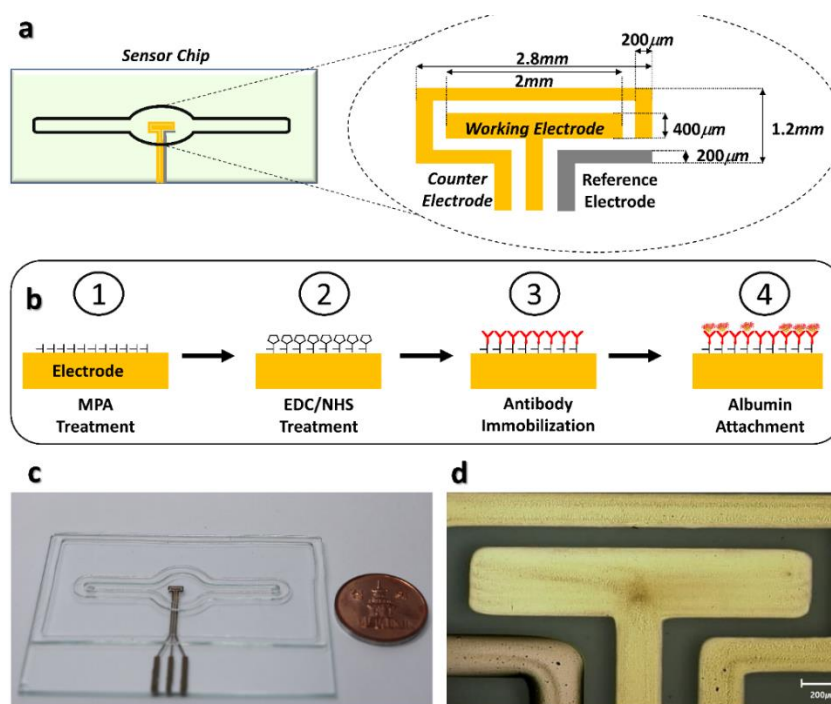


Figure 4. a) Chip schematic and electrode dimensions. b) Surface modifications pattern with immobilization of antibody. c) electrodes in chip assembly with microfluidic channels. d) 50X magnification microscopic picture of electrodes.

b. Electrochemical Analysis

On bare electrodes we performed Cyclic Voltammetry (CV) as a means of faradic redox reaction and Electrochemical impedance spectroscopy (EIS) as a means of sensor immobilization to ensure the redox potential and electrochemical stability of the developed sensor. The voltage range for EIS was maintained at 0.01 V AC and 0.035V as DC Bias with frequency range set from 1 to 5 KHz. The same steps were carried out after the functionalization. The solution composition used for redox prob was 5 mM Potassium ferricyanide in PBS with maintained pH of 7.23 (Sigma®). PalmSens4 in 3-electrode configuration was used to record the measurements and PSTrace5 was used for data acquisition. The faradaic redox reaction and sensor

immobilization are characterized based on the charge transfer resistance. For the CV 200 mV/s was set as scan rate and voltage range set to be from - 0.4 volts to 0.8 volts.

c. Mathematical Derivation

To ensure the real time albumin concentration mathematical modelling was done. The bode plot generated depicted the negative relation between the impedance and concentration of albumin. At the set frequency of 18.087 Hz, admittance was measured later by inverting the measured impedance.

$$Z^{-1} = Y \quad (Eq. 1)$$

Afterwards, the output ΔY was calculated after regular interval of thirty minutes by measuring the change in admittance. Thus the Y is actually the change in admittance after regular time interval as already mentioned. Whereas the albumin concentration and other important parameters were calculated using equation 3.

$$\Delta Y = Y_{Tn} - Y_{Tn-1} \quad (Eq. 2)$$

The next equation calculates " C_{Tn} " of human serum albumin for specific intervals.

$$C_{Tn} = m\Delta + b \quad (Eq. 3)$$

For estimating the total albumin concentration equation was developed. In that, all previous albumin concentrations were added to current concentration at specified intervals.

$$C_{Total} = \sum\{C_{T1}, C_{T2}, C_{T3}, \dots \dots, C_{Tn}\} \quad (Eq. 4)$$

Finally, for both cases the complete albumin concentration was estimated for long-short term experiments.

4.3. OoC Models

4.3.1. Kidney MPS Cell Culture

Cell line derived from immortal epithelial cells from proximal tubule segment of human nephron, HK-2 (ATCC®) and CCD-986sk, human-derived foreskin fibroblasts taken from Korean Cell Line Bank were utilized for the establishment of a mixed culture fibroblast and HK-2 cell line. Respective cell bank recommended media and culture condition were given to the cell and cells were seeded in the MPS platform at the time of 80-90 percent confluency. Before cell seeding in the culture chamber, the glass was coated with the collagen-I protein being used as extracellular matrix (ECM) to create an adhesive surface for cell to form monolayer later on. After ECM coating and cell seeding, the top glass layer was assembled, and chip was placed in chip holder and connected with tubing to circulate media.

Firstly, for 5 days, the cell monolayer was exposed to recommended media type for the development of confluency by the mixed culture of HK-2 cell line and fibroblast cell line. Afterwards to create hyperglycemia mimicking nephrotoxicity condition, high glucose media with 30mM was circulated in the microfluidic channel. Proximal tubule cellular injury condition was developed within a period of 3-4 days. Finally, the monolayer of mixed cells was exposed to the media containing drug to check the recovery of the disease towards normal conditions again. Metformin drug which is a commercially available anti-diabetic and anti-inflammatory agent, was added in media at molarity of 5 mM.

4.3.2. Liver MPS Cell culture

HepG2 and CCD-986sk, were purchased from ATCC and Korean cell line bank, respectively. Cell lines were grown according to the given protocols by cell banks. Similar to kidney chip assembly, liver chip was prepared by adding a coating layer of

collagen-I (Sigma®) for improved cell adhesion. A ratio of 8:2 was used for mixing of HepG2 cells and CCD-986sk cell lines making a total of 100,000 cells. Once the cells are attached to the bottom layer, it was kept in incubator, making them attached in 4 hours. Later, the top layer is installed upon bottom layer for completing the microfluidic system for media circulation. A peristaltic micro-pump was used for connecting immunosensor chip with liver MPS chip and circulating media.

To perform the experiment, a mixed monolayer of hepatocytes and fibroblasts is established to perform experiment. First the company recommended culture media without stimulants is circulated in the system for a period of 48 hours which later is changed with the media containing high glucose media at 30mM molarity to induce hepatopathy and duration of high glucose media for circulation is also kept 48 hours to make a disease model. As the final step, for last two days the media containing drug (metformin) was circulated with the 5mM concentration.

4.4. Biochemical Assays

4.4.1. Viability Assay and ELISA Measurement from Kidney MPS

To take a count of live cells against dead cell, a viability assay was performed using Cytotoxicity/Viability Assessment Kit® from Invitrogen™. Calcein-AM dye and ethidium homodimer-I dye were applied for assessing live and dead cells. Ethidium homodimer enters the dead cell and show reddish color illumination at excitation of ~495 normal media and emission of ~635 normal media) whereas Calcein-A enters live cell and shows a greenish color fluorescence with the excitation range of 495 normal media and emission range of 515 normal media.

Additionally, for quantifying HSP70 protein and KIM-1 protein concentration in the media, ELISA assays were performed using the commercial kits i.e., KIM-1 ELISA Kit, Abcam and HSP70 ELISA Kit Invitrogen. A protocol according to the

manufacturers' provided manual was used and a microplate reader was used to check the end-point absorbance values and protein concentration was derived in the media.

4.4.2. Albumin, Urea, and P450 Assays

Media was stored after each interval of short and long experiment for the albumin sensor evaluation i.e., 8 hours interval of 24-hour experiment and 1 day interval for 6 days and stored at -80° degree centigrade. ELISA kit for albumin was purchased from Abcam and ELISA assay was done according to the manual given by manufacturer. The process of concentration normalization was performed to manage the values after each media change. For urea assay, Abnova's urea assay kit was purchased, and assay was performed according to the manufacturer's protocol.

P450 assay was purchased from Promega. A 2-day long interval was selected for the enzyme activity measurement after the completion of each experimental phase and performed according to the manufacturer's protocol in a clear-bottom 96 wells. Lastly, microplate reader was used to check the fluorescence intensity of each sample.

4.4.3. Immuno-fluorescence Staining

For the justification of albumin secretion from hepatocytes, an end-point immunostaining is done at the termination of microfluidic experiment. Firstly, hepatocytes and fibroblasts are fixed using a 4% solution of paraformaldehyde at RT for 15 mins. Later, for 15 mins, 0.1% Triton X-100 in PBS is added on the cell to make them permeable and a BSA solution of 3% is treated for 1 hour at RT. Cells are treated with primary antibody of albumin for overnight at 4° C. After an overnight incubation period, the cells monolayer is treated with secondary antibody with conjugated Alexa Fluor according to the provided concentration by the manufacturer for 60 mins. Lastly, DAPI stain with 1:5000 dilution is added upon the cells for staining nucleus of cells. Microscopic pictures were captured using fluorescence microscope.

4.5. Computational Fluid Simulation

An art of observing and analyzing the underlying patterns in fluid flows using computational tools is called computational fluid dynamics (CFD). The applications of the CFD range from aerodynamics profiling for the purpose of design modification to micro-fluidic analysis of fluid patterns in organ on chips. The application of CFD in organ on chip (OOC) can be expanded to critically analyzing the temperature, pressure, and flow distribution in the micro-fluidic channel of the organ on chip. For the present study, two different designs of the OOC with sensors and without sensors using 3D designing SolidWorks Software were made. First of all, microfluidic channels were created on the lower layer of the chip and then the top glass with exact dimensions is extruded. While the simulation was performed using COMSOL Multi-Physics 5.1. During the simulation the material for the channels were declared as silicon glass to mimic the practical experimentation as closely as possible. To study the flow distribution a pre-defined internal flow rate of 60 ul/min was set for fluid.

4.6. Statistical Analysis

Each data point was generated when the experiments were carried out in duplicate. Two chips were dedicated in every experiment to create the duplicated data. The comparison between the generated data was made in 2-way ANOVA and the results were presented as means \pm standard error of the means (sem) of 3 independent experiments.

5. Results

Chronic diseases such as hypertension and diabetes influence an imbalanced function of kidney and leading to nephrotoxic and hepatotoxic conditions. Higher glucose levels in blood serum leading towards the development of albuminuria condition in proximal tubule causing tubulopathy (61). The building material for MPS was carefully selected including glass, ITO electrodes and silicone elastomer to print channels (62-64). The glass-based chips are preferable as glass eliminates the potential absorption of molecules in the microfluidic channel (65).

5.1. Kidney MPS with TEER Sensor

5.1.1. Proximal Tubule Cells and Fibroblasts Mixed Culture

Firstly, the mixed culture of fibroblasts with HK-2 cells was performed till first 5-day period for the development of a confluent monolayer to mimic proximal tubule. After first day of microfluidic cell culture when cells were seen to be settled and started dividing, an exponential rise of impedance graph depicted cell proliferation from 2nd day to 4th day. After the formation of a confluent monolayer, a static pattern of impedance was seen on the fifth day of experimentation. Overall, impedance graph trend showed the normal cell proliferation phases i.e., lag phase (cells adjust to environment and start division), log phase (an exponential rise in cell number) and stationary phase (cell growth equals cell death and cell number remains approximately same) as shown in Fig. 3.

5.1.2. Inflammatory Nephrotoxicity

Secondly, after first 5 days of normal media culture, it was replaced with media containing stimulant (high glucose, 30 mM) to cause nephrotoxicity by cell damage. After the exposure of cells to high glucose, for initial 4 days, impedance graph showed a steady trend of decreased values which indicated the disruption of tight-junction

proteins. Similar to 1st phase of experimentation with normal media, high glucose showed a same trend in impedance graph on 5th day with a static phase and showing stability and resistance of cell towards high glucose media. In such condition, a disease model of renal diabetic nephrotoxicity was established for further treatment with drug. Additionally, pH monitoring of the cell culture was also performed to detect the development of acidic environment which can be linked to the inflammatory responses of cells (66). In the last step of kidney MPS experimentation a media containing anti-inflammatory drug is circulated for restoring the cell towards normal condition.

5.1.3. Drug Treatment

At the final phase of experiment, Metformin drug was circulated in kidney MPS for the restoration of tight-junction proteins. A steady increase in the TEER graph was observed after the administration of drug indicating the recovery of cells monolayer from cell injury. TEER value measurements showed significant information regarding the cell growth pattern. Comparable to TEER values, a decreasing trend of media pH can be seen further validating the TEER data which was in relevance with disease development and disease treatment upon drug administration. A relative change of pH values with the circulation of media with high glucose and circulation of media with drug further highlights the reliability of kidney MPS for drug and disease analysis. Pictures captured by microscope integrated in the kidney MPS show a monolayer development on the fifth day of experiment, then after inflammation development on the tenth day of experiment and lastly recovery from disease on the fifteenth day are represented in Fig. 5. Cells displayed growth into monolayer during the first experimental phase which later was reduced due to the cell damage induced by high glucose media and lastly the reduction in inflammation was seen with positive outcomes of drug treatment (Fig.5). Despite of the restoration of tight-junction proteins

across the cell walls was not similar to the natural level which was achieved in first 5 days with normal media, yet the results were significantly improved from the disease condition.

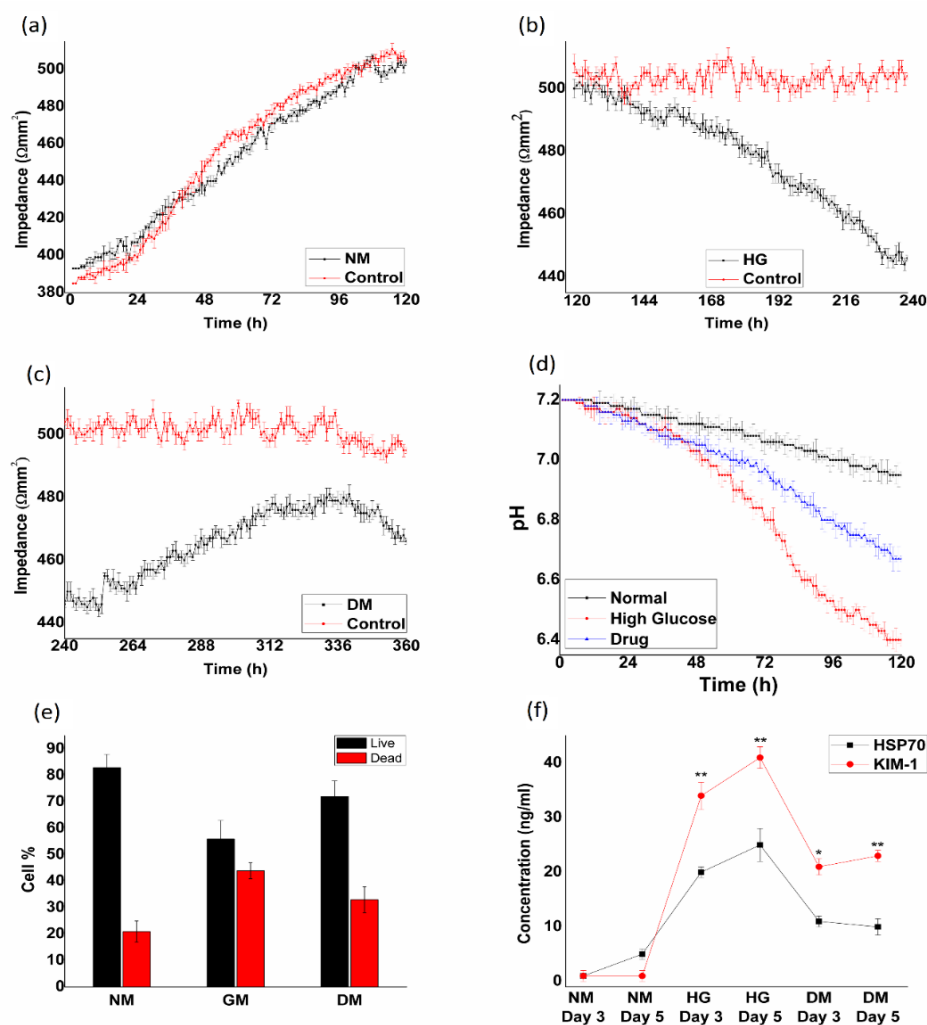
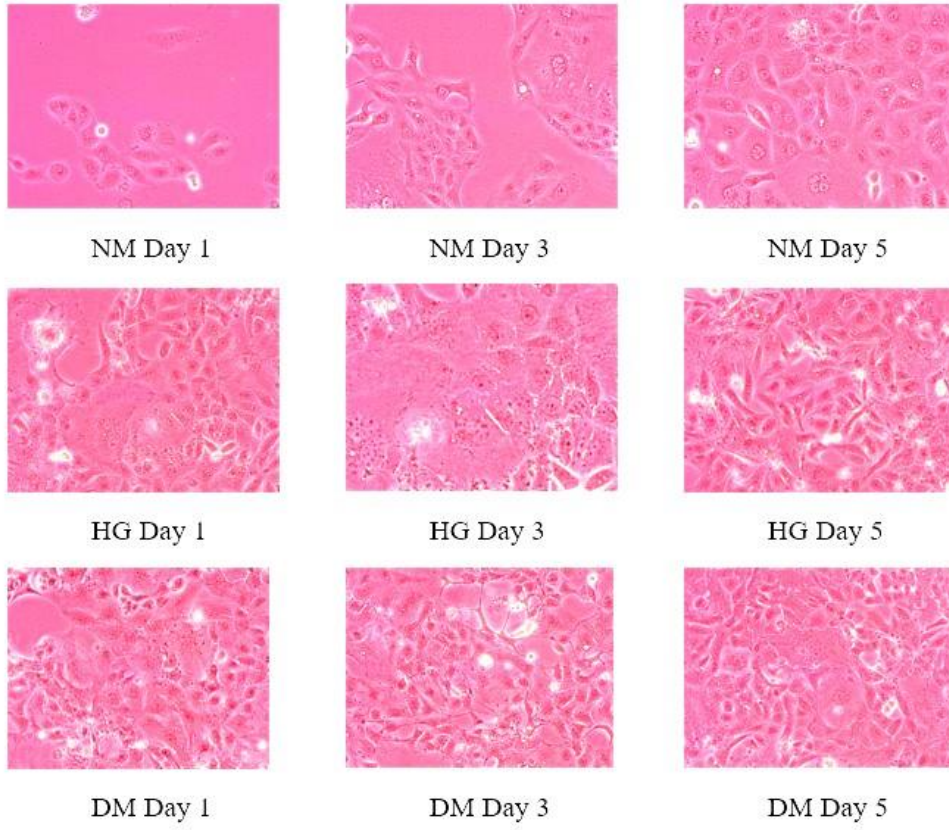


Figure 5. Relative Result of TEER sensor in multiple conditions. (a). Impedance graph for cells after treatment of normal media. (b). Impedance graph for cells after treatment of glucose containing media. (c). Impedance graph for cells after treatment of drug containing media. (d). pH measurement for relative pH trend in normal media, high glucose media and drug-containing media for 5 days. (e). Live-Dead Assay results for cells under normal media, high glucose media and drug-containing media. (f). ELISA results for protein biomarkers.

(a) Light Microscopy



(b) Platform Integrated Microscope

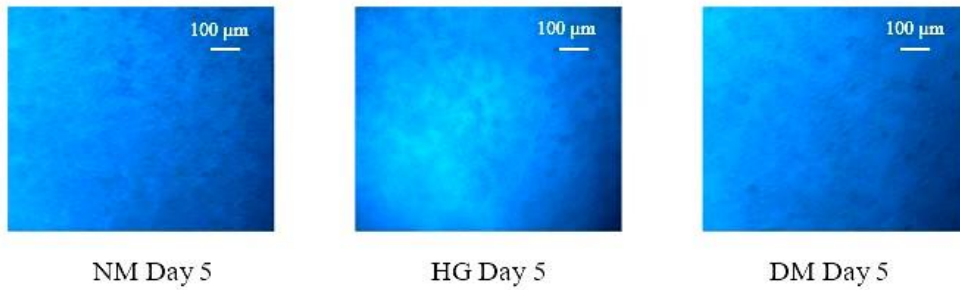


Figure 6. Light microscopy pictures of fibroblast and HK-2 cells. (a) Normal media represented good confluent monolayer of cells. (b) Microscopic Images from platform integrated microscope with an interval of five days of incubation with normal media, high glucose media and drug-containing media (scale bar is 100 μ m, and pictures are captured at 100X).

5.1.4. Viability Analysis

Cell viability assay was performed, and pictures were taken by confocal microscope in which dead cells are represented with red dye (ethidium homodimer) and live cells are represented by Calcein-AM (Fig. 7). The collected pictures were run through the analytic software for image processing “ImageJ” which estimated the viability of cells in per percent. The average viability count fell in a range above 80 % in normal media. Cell viability decreased to lower than 60 % with the treatment of high glucose media for a 5-day duration, which later on increased above the percentage of 70 with the drug again for 5-day duration (Fig. 5f).

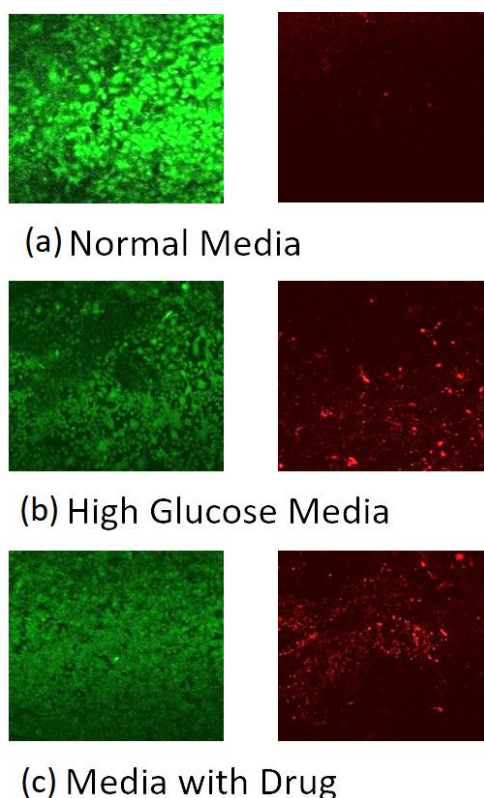


Figure 7. Representative pictures of cell viability assay using confocal microscopy.

5.1.5. KIM-1 and HSP70 ELISA Measurements

The protein biomarkers i.e., KIM-1 and HSP70 were measured using ELISA assay kits according to the manufacturer's protocol. The concentrations of each protein were measured after the interval of each phase of the experiment in kidney MPS (Fig. 8). Elevated secretions of KIM-1 and HSP70 have shown a direct link with the development of inflammatory condition in the kidney MPS and its feasibility to be used as a disease model for drug treatment (67). An insignificant trend of KIM-1 and HSP70 release was observed in the first phase of experiment during the treatment with normal media. Both the protein biomarkers represented a significant upsurge as the kidney MPS was treated with high-glucose media for development of inflammatory condition. The selected biomarkers successfully validated the development of disease condition and disease recovery as well as coincided with the TEER sensor values further affirming the role of TEER sensor to assess the cell confluency. Elevated expression of biomarkers affirmed necrosis and cell stress developed with exposure of high glucose media. In the same way, as the drug containing media was circulated in the system a decline in the stress signal was seen and it was also indicated by the protein biomarkers.

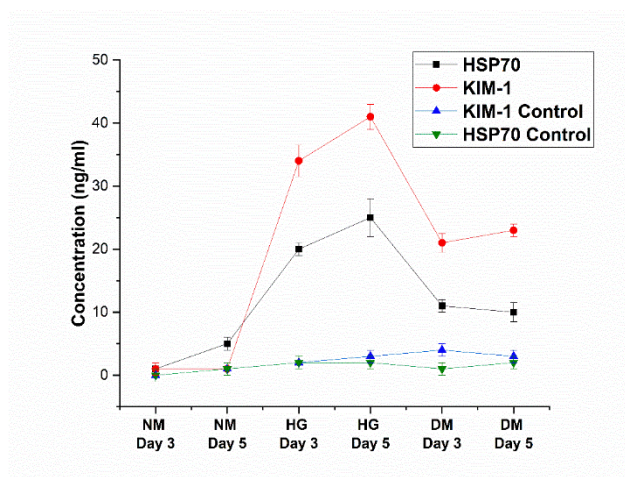


Figure 8 ELISA result of KIM-1 and HSP70 proteins. In each experimental phase, media was stored from 3rd and 5th day i.e., normal media, high glucose, and drug media. Concentrations shown in mean \pm S.E.M.

5.2. Liver MPS with Albumin Immunosensor

5.2.1. Electrochemical Analysis of Human Serum Albumin Sensor

For determining the electrode stability CV was conducted at first and then resistor (R_{ct}) of the sensor was measured using the EIS at various concentration from 1 ng to 1 μg . The results depicted the reproducibility in 5 consecutive cycles as shown in figure 9a. The Nyquist plot developed because of spectral curves from the given concentrations showed the observable difference in impedance. The relation between the solution concentration and impedance is inversely proportional. The mathematical modelling was also performed for continuously ensuring the differences in EIS recorded by the PALMSENS.

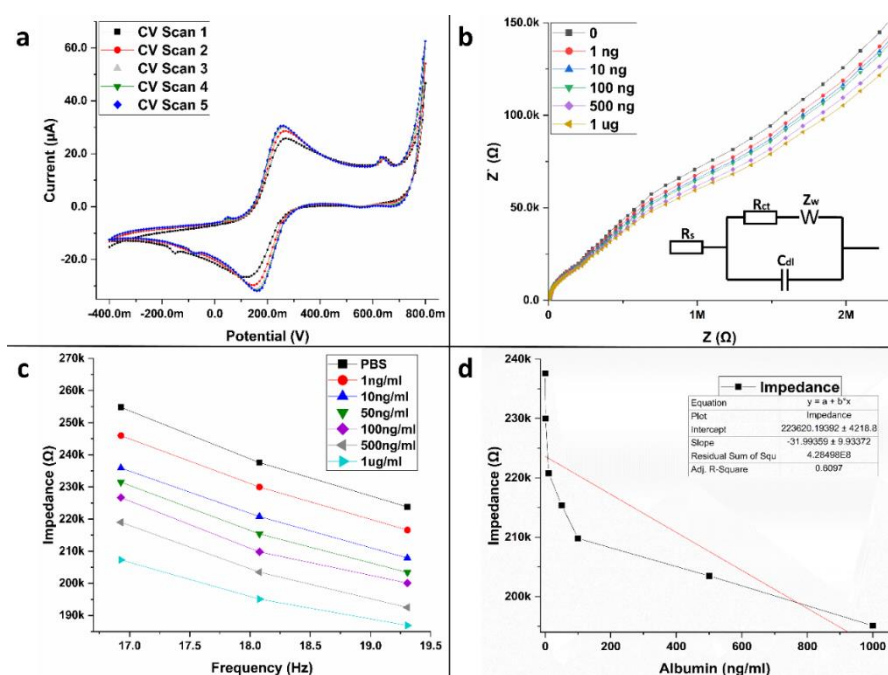


Figure 9. Sensor Characterization a) plot showing the stability of the sensor because of CV test b) Plot showing the testing results for confirming the R_{ct} of the sensor c) Plot showing the relation between frequency and impedance. d) Curve at given frequency of 18.078 Hz for calibrating the sensor.

5.2.2. Liver MPS Design

Liver MPS design consisted of sensor-chip, liver-chip, and reservoir for media connected by the tubing through a peristaltic pump to keep the circulation of media.

Additionally, a bubble trap was adjoined to the tubing to keep the formation of bubbles in the minimum range. The box in which liver MPS was set up contained temperature control and CO₂ control to keep the conditions similar to a cell culture incubator for proper growth of cells. Liver MPS was established and then albumin immunosensor was attached for continuous measurement of the albumin in the media. Liver MPS with immunosensor-chip were designed to be portable for making its replacement easier and swift and also the functional perspective of liver cells was not affected by the presence of sensor. For the testing of sensor, the experimental parameters were divided into 2 categories i.e., short-term (24 hours) experiment and long-term (6-days), to monitor the performance of sensor in different circumstance and checking the working of sensor.

5.2.3. Sensor Testing for 24 Hours

First, the sensor was examined in 1-day long experimentation to affirm the sensor results. A confluent monolayer of mixed culture of hepatocytes and fibroblasts was prepared in a chip and attached to the sensor for 24 hours to mimic liver microenvironment. The 24 hours long experiment was further divided into 3 phases of 8 hours. First 8 hour interval included media circulation without any stimulant, second 8 hours included the circulation of media containing the stimulant interleukin 1-beta (IL-1 β) which is a pro-inflammatory cytokine (68, 69), third 8-hour phase included the normal media circulation again without any stimulant. First phase was used to start the microfluidic culture, second phase was used for the causing of inflammation and third phase referred to as a recovery phase from disease. The albumin concentration values were taken from immunosensor after each interval of 30 minutes. Then, the albumin concentration was represented in two ways, one was albumin concentration at a specific given time of measurement and second the albumin concentration added up from the start (Fig. 4). The albumin immunosensor was successfully monitoring the continuous

changes in the albumin concentrations in the media which were later confirmed using the ELISA measurements (Fig. 5).

5.2.4. Sensor Testing for 6 Days

For the 6 days long experimentation of albumin immunosensor in liver MPS, similar parameters to short-term experiment were selected, i.e., already prepared liver-chip with the mixed culture of cells was attached to the freshly prepared immunosensor. The sequence of long-term experimentation included first media exposure for 2 days without any stimulant. Later, liver MPS was treated with high glucose media (30 mM) for next 2 days to develop a condition of diabetic hepatopathy. Lastly, liver MPS was treated with media containing metformin drug to restore the cell injury caused by high glucose media. As expected, the albumin secretion pattern was according to the circumstances starting with a steady rise then a sudden decline due to inflammation and later recovery upon treatment with drug. The continuous and quick response from sensor was successfully monitoring the development of disease and disease recovery upon the treatment of drug.

To determine reference values for albumin production in normal cell condition, experimentation was done without any interference of stimulants for same period as short-term and long-term experiments in liver MPS. It was visible from the data that minor differences in albumin concentrations upon the treatment with stimulants and drug, the sensor successfully measured albumin secretion. The interval based specific albumin concentrations and total concentration were compared to the reference (Fig. 4). Moreover, the interval-based and total concentrations of the albumin at different time-points were also compared with the albumin ELISA measurements were in acceptable range of the sensor provided vales further validating sensor data (Fig. 5).

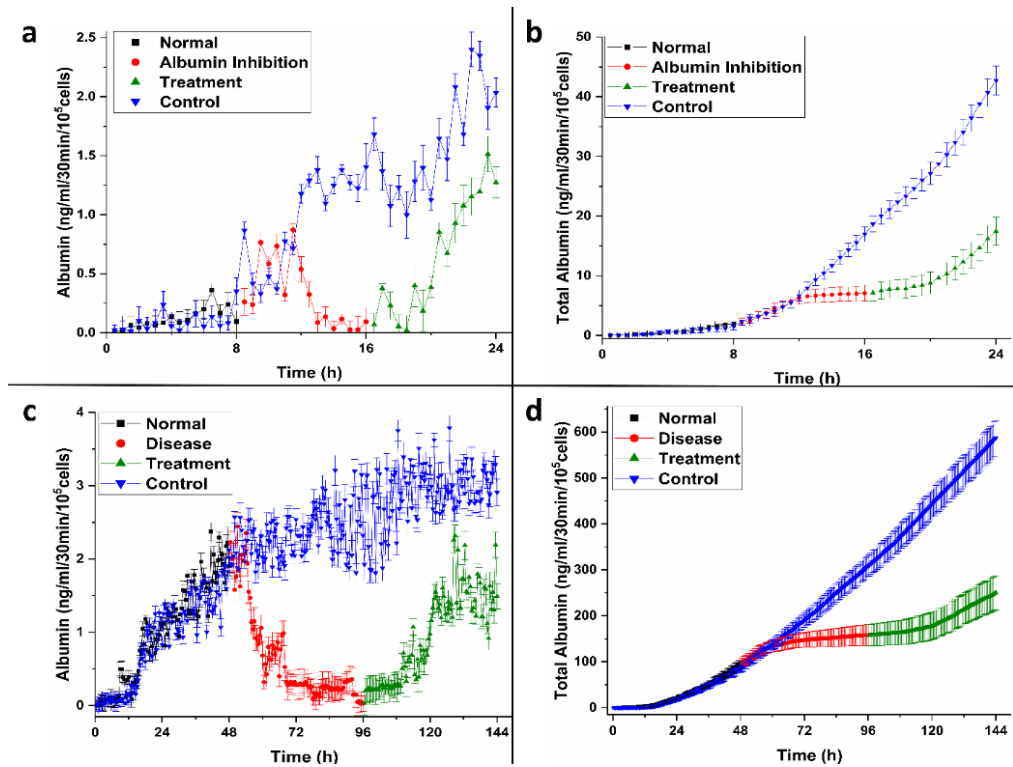


Figure 10. Immunosensor Measurements. a) Specific albumin concentrations at specific time-points in 24-hour experiment. b) Total albumin concentrations at specific time-points in 24-hour experiment. c) Specific albumin concentrations at specific time-points in 6-day experiment. d) Total albumin concentrations at specific time-points in 6-day experiment.

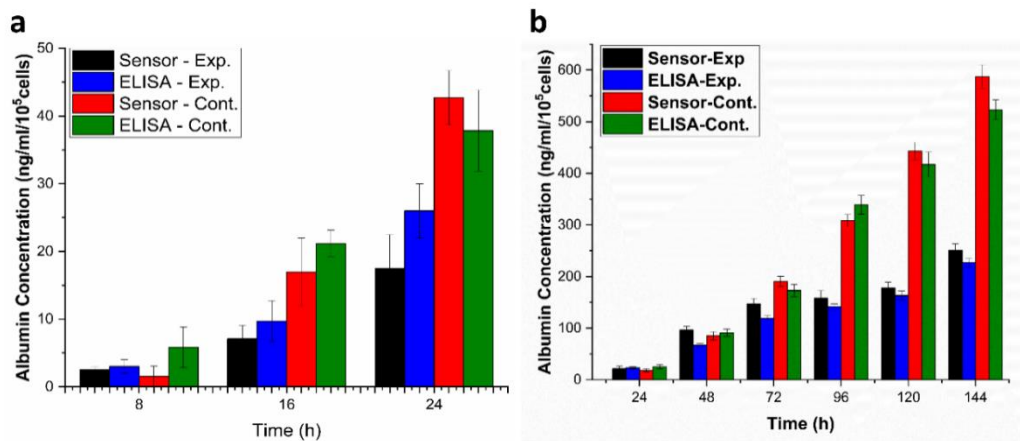


Figure 11. A comparison of albumin concentration measurements taken by immunosensor versus ELISA kit. a) 24-hour experiment result. b) 6-day experiment result

5.2.5. Biochemical Measurements

Bioassays represented treatment of the developed disease consistently verifying function of sensor. Additionally, chip model was compared with traditional 2D cell culture for analyzing the benefit MPS. Biochemical assays such as, P450(3A4) activity, albumin measurement, and urea measurements were chosen to analyze the liver-chip. Fig. 13a shows significantly different reading between experimental chip versus control chip for albumin protein. Concurrently, a significant difference was found in 3D versus 2D cell culture systems, strengthening the idea of improved microphysiological similarity to human. Urea analysis in Fig. 13b represented analogous pattern from the start of experimentation which later on changed during treatment of drug and urea measurements showed significantly different secretion pattern in MPS in comparison with 2D platform. Likewise, P450 activity assay given in Fig.13c showed significance in 3D cell culture chip versus 2D cell culture of HepG2 cell line. A significant decline in the activity of cytochrome P450 was observed while the development of disease in liver MPS however other experimental conditions represented a similar to control activity of P450 for 3D versus 2D system. Furthermore, immunofluorescence staining as shown in Fig. 12 confirmed secretion of albumin. Albumin expression analysis done by immunostaining showed a greater expression for long-term experiment in comparison with short-term experimentation. Control conditions for the experiment showed an improved staining of albumin at the end point showing more albumin production in comparison with experimental conditions.

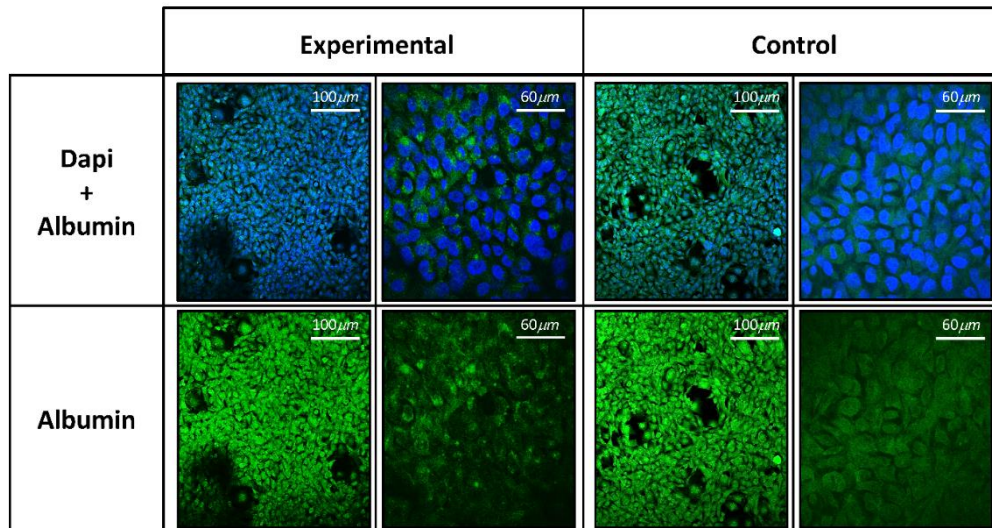


Figure 13. Fluorescence Microscopy for albumin staining at termination of 6 days long experiment. Microscopy results are aligned with other molecular assay and sensor analysis further affirming the development of disease and recovery model.

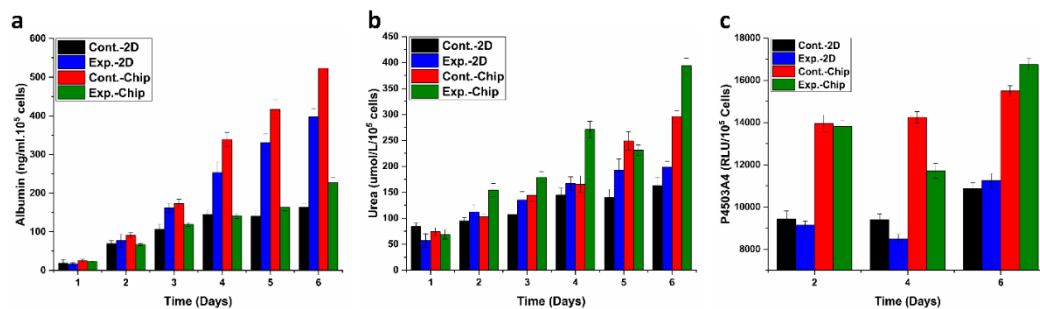


Figure 12. Molecular biomarker results, Chip denotes Liver MPS and 2D denotes petri dish a) comparison of albumin secretion between 3D and 2D culture. b) comparison of urea excretion between 3D and 2D culture. c) comparison of P450 activity between 3D and 2D culture.

5.2.6. Fluid Dynamics Simulation

CFD study was performed for two cases; In the first part, sensors were not included and in the second part sensors were included. Both simulation cases were performed in COMSOL Multiphysics 5.1. The geometry dimensions for simulation and experiments were kept same. Focus of the CFD study was to observe the flow and pressure trajectories at various points in channel. The fluid was declared as cell culture media with predefined flow rate of 60 $\mu\text{l}/\text{min}$. The variation in the pressure and flow

are shown with change in color of the trajectories. Here the red color shows the highest pressure and blue color shows the lowest as shown in Fig. 14

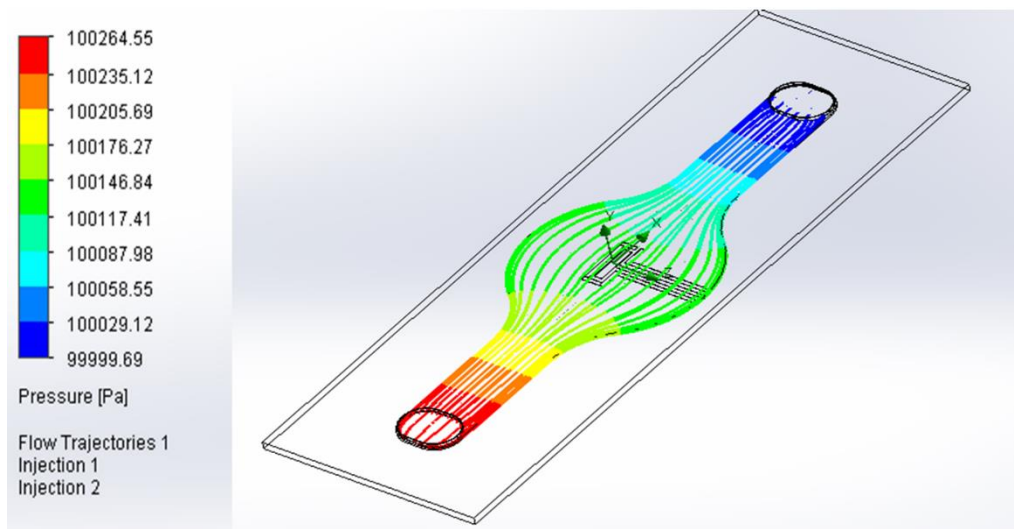


Figure 14. Simulation results of computational fluid flow analysis in the microfluidic channel (pressure scale shown on left).

6. Discussion

Modern innovations in MPS tools are providing initial developments to replace animals for drug development studies. The developed kidney and liver MPS platforms offer the possibility of continuous measurements of cellular growth pattern. Average impedance measurements taken from TEER exhibited the development of increased capacitive resistance with passage of time as cell monolayer was formed and a directly proportional pattern with cell proliferation was visible for impedance readings. Kidney-chip showed a rise in cell damage upon exposure with high glucose media. A continuous measurement of cell injury was validated by TEER sensor for 5 day long period. Kidney injury molecule (KIM-1) and heat-shock protein (HSP70) showed similar increase in their concentration with the development of inflammation. A subsequent exposure of anti-inflammatory drug was given and TEER measurements were taken and confirmed by KIM-1 and HSP70 ELISA reading with an additional viability study. Liver-chip provided the cellular environment with an incessant response for the development of disease model and showed a restoring phenomenon of normal growth upon drug treatment perfectly measured by albumin immunosensor. It can be inferred that both the sensor, TEER sensor for kidney MPS and albumin sensor for liver MPS showed reliable monitoring. Recently, the models for proximal tubule have shown ability to imitate disease and normal conditions. The currently developed liver MPS and kidney MPS have the advantage of material as glass-based chip showed no absorption of drug molecules which has been observed in PDMS-based chips.

Albumin immunosensor validation was done by 2 experimental methods. Firstly, for 1 day and secondly for 6 days. The 24 hour experiment consisted of three 8 hour intervals with first 8 hours being exposed to normal media then exposure of interleukin 1β for 8 hours and finally normal media exposure for last 8 hours. For 6 days long

experimentation, first, a confluent layer of cells was developed for 2 days with later exposure of high glucose for modeling disease for 48 hours and lastly, for 2 days metformin (anti-inflammatory and anti-diabetic drug) was treated. Metabolic assays showed relevance to albumin secretions. After a normal rise in albumin secretions, liver-chip showed a decrease in concentration of with the exposure of high glucose media. Moreover, a declining pattern in the activity of P450(3A4) which was quantified with 2-day intervals whereas urea concentration showed a rise with declining albumin value. Eventually upon drug treatment, P450 activity and albumin secretion showed recovery whereas urea concentration showed a decline. Albumin immunosensor successfully measured continuous fluctuations of albumin concentration showing drug and disease analysis. Favorably, current measurement capability of sensor was not influenced by cellular proliferation and the sensor remained functional for 6 days. Both of the experiments showed similar patterns for the albumin secretions. An instant response was measured by the immunosensor for albumin readings.

Both the sensors are embedded in the MPS model for the first time and glass chips have been found to be a strong substrate for electrode printing. The developed microfluidic platforms hold the potential to improve the field of organ-chips. The metabolite and cell monolayer measurements in a continuous manner will improve the drug discovery and development studies with a faster data acquisition.

7. Conclusion and Future Perspectives

The kidney MPS successfully monitored continuous TEER value with the integrated sensors exhibiting cell injury and drug efficacy. The liver MPS to measure the development of diabetic hepatopathy and drug assessment in conjunction with combined albumin immunosensor was efficiently established. MPS platforms are efficient due to their swift capacity to model disease with continuous online measurements in a reduced time-period. Simultaneously, the MPS platforms present the clinical prediction of drug results for future use in clinical trials. Albumin measurement in continuous manner for a longer period of time may enhance the predicting capacity and lead to a large-scale analysis of drugs quickly. The precision of hepatic and renal MPS platforms for mimicking the process of disease modeling and recovery modeling after treatment of drug treatment was effectively substantiated continuous measurements through sensors. The end-point biochemical assays were totally in correlation with the sensor data further verifying the accuracy of sensor development. Another advantage of microfluidic immunosensor is its portability and compatibility with other peristaltic pump based microfluidic MPS platforms. Both the platforms consist of glass-based chip design eventually overcoming the limitation of drug and molecular absorption presented by the PDMS based chips. Overall, microfluidic MPS platforms present the capacity to mimic human organs and tissues with effectiveness to replace the usage of animal models. The clinical predictive capacity of MPS platforms will speed-boost the drug discovery and development pipeline. The embedded sensors with the potential to continuously monitor the cellular microenvironment further strengthen MPS performance.

References

1. Taylor MW. A History of Cell Culture. *Viruses and Man: A History of Interactions*. Cham: Springer International Publishing; 2014. p. 41-52.
2. Shama G. The “Petri” dish: a case of simultaneous invention in bacteriology. *Endeavour*. 2019;43(1-2):11-6.
3. Chethikkattuveli Salih AR, Hyun K, Asif A, Soomro AM, Farooqi HMU, Kim YS, et al. Extracellular Matrix Optimization for Enhanced Physiological Relevance in Hepatic Tissue-Chips. *Polymers*. 2021;13(17):3016.
4. Kim Y-S, Asif A, Chethikkattuveli Salih AR, Lee J-W, Hyun K-N, Choi K-H. Gravity-Based Flow Efficient Perfusion Culture System for Spheroids Mimicking Liver Inflammation. *Biomedicines*. 2021;9(10):1369.
5. Salih ARC, Farooqi HMU, Kim YS, Lee SH, Choi KH. Impact of serum concentration in cell culture media on tight junction proteins within a multiorgan microphysiological system. *Microelectronic Engineering*. 2020;232:111405.
6. Asif A, Khalid M, Manzoor S, Ahmad H, Rehman AU. Role of purinergic receptors in hepatobiliary carcinoma in Pakistani population: an approach towards proinflammatory role of P2X4 and P2X7 receptors. *Purinergic Signalling*. 2019;15(3):367-74.
7. Asif A, Manzoor S, Tuz-Zahra F, Saalim M, Ashraf M, Ishtiyag J, et al. Zika virus: immune evasion mechanisms, currently available therapeutic regimens, and vaccines. *Viral immunology*. 2017;30(10):682-90.
8. Asif A, Park SH, Soomro AM, Khalid MAU, Salih ARC, Kang B, et al. Microphysiological system with continuous analysis of albumin for hepatotoxicity modeling and drug screening. *Journal of Industrial and Engineering Chemistry*. 2021;98:318-26.
9. Jordheim LP, Durantel D, Zoulim F, Dumontet C. Advances in the development of nucleoside and nucleotide analogues for cancer and viral diseases. *Nature reviews Drug discovery*. 2013;12(6):447-64.
10. Baudy AR, Otieno MA, Hewitt P, Gan J, Roth A, Keller D, et al. Liver microphysiological systems development guidelines for safety risk assessment in the pharmaceutical industry. *Lab on a Chip*. 2020;20(2):215-25.
11. Seok J, Warren HS, Cuenca AG, Mindrinos MN, Baker HV, Xu W, et al. Genomic responses in mouse models poorly mimic human inflammatory diseases. *Proceedings of the National Academy of Sciences*. 2013;110(9):3507-12.
12. Grubb ML, Caliri SR. Fabrication Approaches for High-Throughput and Biomimetic Disease Modeling. *Acta Biomaterialia*. 2021.
13. Hsia GSP, Esposito J, da Rocha LA, Ramos SLG, Okamoto OK. Clinical Application of Human Induced Pluripotent Stem Cell-Derived Organoids as an Alternative to Organ Transplantation. *Stem Cells International*. 2021;2021.
14. Khan SR, Al Rijjal D, Piro A, Wheeler MB. AI-integration and plant-based traditional medicine for drug discovery. *Drug discovery today*. 2021.
15. Aldewachi H, Al-Zidan RN, Conner MT, Salman MM. High-throughput screening platforms in the discovery of novel drugs for neurodegenerative diseases. *Bioengineering*. 2021;8(2):30.
16. Asif A, Kim KH, Jabbar F, Kim S, Choi KHJM, Nanofluidics. Real-time sensors for live monitoring of disease and drug analysis in microfluidic model of proximal tubule. 2020;24(6).

17. Kimura H, Sakai Y, Fujii T. Organ/body-on-a-chip based on microfluidic technology for drug discovery. *Drug metabolism and pharmacokinetics*. 2018;33(1):43-8.
18. Blume-Kohout ME, Sood N. Market size and innovation: Effects of Medicare Part D on pharmaceutical research and development. *Journal of public economics*. 2013;97:327-36.
19. Rudrapal M, Khairnar J, Jadhav G. Drug repurposing (DR): an emerging approach in drug discovery. *Drug Repurposing Hypothesis Mol Asp Ther Appl*. 2020.
20. Lazonick W, Hopkins M, Jacobson K, Sakinç ME, Tulum Ö. US pharma's financialized business model. *Institute for New Economic Thinking Working Paper Series*. 2017(60).
21. McPherson KC, Shields CA, Poudel B, Fizer B, Pennington A, Szabo-Johnson A, et al. Impact of obesity as an independent risk factor for the development of renal injury: implications from rat models of obesity. *American Journal of Physiology-Renal Physiology*. 2019;316(2):F316-F27.
22. Torkamani N, Churilov L, Robbins R, Jerums G, Beik V, Radcliffe N, et al. Diabetes and higher HbA1c levels are independently associated with adverse renal outcomes in inpatients following multiple hospital admissions. *Journal of Diabetes and its Complications*. 2020;34(1):107465.
23. Zeni L, Norden AG, Cancarini G, Unwin RJ. A more tubulocentric view of diabetic kidney disease. *Journal of nephrology*. 2017;30(6):701-17.
24. Boularaoui S, Al Hussein G, Khan KA, Christoforou N, Stefanini C. An overview of extrusion-based bioprinting with a focus on induced shear stress and its effect on cell viability. *Bioprinting*. 2020:e00093.
25. Qin X, Li J, Sun J, Liu L, Chen D, Liu Y. Low shear stress induces ERK nuclear localization and YAP activation to control the proliferation of breast cancer cells. *Biochemical and biophysical research communications*. 2019;510(2):219-23.
26. Nguyen P, Leray V, Diez M, Serisier S, Bloc'h JL, Siliart B, et al. Liver lipid metabolism. 2008;92(3):272-83.
27. Dehne E-M, Hasenberg T, Marx UJFSO. The ascendance of microphysiological systems to solve the drug testing dilemma. 2017;3(2):FSO0185.
28. Ehrlich A, Duche D, Ouedraogo G, Nahmias YJArobe. Challenges and opportunities in the design of liver-on-chip microdevices. 2019;21:219-39.
29. Low LA, Mummery C, Berridge BR, Austin CP, Tagle DA. Organs-on-chips: into the next decade. *Nature Reviews Drug Discovery*. 2021;20(5):345-61.
30. Broutier L, Mastrogiovanni G, Verstegen MM, Francies HE, Gavarró LM, Bradshaw CR, et al. Human primary liver cancer-derived organoid cultures for disease modeling and drug screening. 2017;23(12):1424.
31. Lancaster MA, Knoblich JAJ. Organogenesis in a dish: modeling development and disease using organoid technologies. 2014;345(6194).
32. Lee H, Chae S, Kim JY, Han W, Kim J, Choi Y, et al. Cell-printed 3D liver-on-a-chip possessing a liver microenvironment and biliary system. 2019;11(2):025001.
33. Kim Y, Kang K, Jeong J, Paik SS, Kim JS, Park SA, et al. Three-dimensional (3D) printing of mouse primary hepatocytes to generate 3D hepatic structure. 2017;92(2):67-72.
34. Li L, Gokduman K, Gokaltun A, Yarmush ML, Usta OBJN. A microfluidic 3D hepatocyte chip for hepatotoxicity testing of nanoparticles. 2019;14(16):2209-26.
35. Esch MB, Ueno H, Applegate DR, Shuler MLJLoaC. Modular, pumpless body-on-a-chip platform for the co-culture of GI tract epithelium and 3D primary liver tissue. 2016;16(14):2719-29.

36. Gori M, Simonelli MC, Giannitelli SM, Businaro L, Trombetta M, Rainer AJPO. Investigating nonalcoholic fatty liver disease in a liver-on-a-chip microfluidic device. 2016;11(7):e0159729.
37. Kang T, Park C, Meghani N, Tran TT, Tran PH, Lee B-JJP. Shear Stress-Dependent Targeting Efficiency Using Self-Assembled Gelatin–Oleic Nanoparticles in a Biomimetic Microfluidic System. 2020;12(6):555.
38. Feldmann G, Penaud-Laurencin J, Crassous J, Benhamou JJG. Albumin synthesis by human liver cells: its morphological demonstration. 1972;63(6):1036-48.
39. Greenblatt D, Koch-Weser JJEjocp. Clinical toxicity of chloridazepoxide and diazepam in relation to serum albumin concentration: A report from the Boston collaborative drug surveillance Program. 1974;7(4):259-62.
40. Yang F, Bian C, Zhu L, Zhao G, Huang Z, Huang MJJosb. Effect of human serum albumin on drug metabolism: structural evidence of esterase activity of human serum albumin. 2007;157(2):348-55.
41. Levitt DG, Levitt MDJIjogm. Human serum albumin homeostasis: a new look at the roles of synthesis, catabolism, renal and gastrointestinal excretion, and the clinical value of serum albumin measurements. 2016;9:229.
42. David SAJEih, disease HB, SM Opal, SN Vogel,, DC Morrison e. The interaction of lipid A and lipopolysaccharide with human serum albumin. 1999:413-22.
43. Bertucci C, Domenici EJCmc. Reversible and covalent binding of drugs to human serum albumin: methodological approaches and physiological relevance. 2002;9(15):1463-81.
44. Zheng CM, Wu CC, Lu CL, Hou YC, Wu MS, Hsu YH, et al. Hypoalbuminemia differently affects the serum bone turnover markers in hemodialysis patients. 2019;16(12):1583.
45. Rebelo R, Barbosa AI, Caballero D, Kwon IK, Oliveira JM, Kundu SC, et al. 3D biosensors in advanced medical diagnostics of high mortality diseases. 2019;130:20-39.
46. Meghani N, Kim KH, Kim SH, Lee SH, Choi KH. Evaluation and live monitoring of pH-responsive HSA-ZnO nanoparticles using a lung-on-a-chip model. Archives of Pharmacal Research. 2020;43(5):503-13.
47. Riahi R, Shaegh SAM, Ghaderi M, Zhang YS, Shin SR, Aleman J, et al. Automated microfluidic platform of bead-based electrochemical immunosensor integrated with bioreactor for continual monitoring of cell secreted biomarkers. 2016;6(1):1-14.
48. Vitorino R, Guedes S, Costa JPd, Kašička V. Microfluidics for peptidomics, proteomics, and cell analysis. Nanomaterials. 2021;11(5):1118.
49. Fu Y, Zhang Y, Khoo BL. Liquid biopsy technologies for hematological diseases. Medicinal Research Reviews. 2021;41(1):246-74.
50. Cloet T, Momenbeitollahi N, Li H. Recent advances on protein-based quantification of extracellular vesicles. Analytical Biochemistry. 2021:114168.
51. Ji H, Qin W, Yuan Z, Meng F. Qualitative and quantitative recognition method of drug-producing chemicals based on SnO₂ gas sensor with dynamic measurement and PCA weak separation. Sensors and Actuators B: Chemical. 2021;348:130698.
52. Yang Z, Albrow-Owen T, Cai W, Hasan T. Miniaturization of optical spectrometers. Science. 2021;371(6528).
53. Stetter JR, Li J. Amperometric gas sensors a review. Chemical reviews. 2008;108(2):352-66.

54. Ahmad R, Griffete N, Lamouri A, Felidj N, Chehimi MM, Mangeney C. Nanocomposites of gold nanoparticles@ molecularly imprinted polymers: chemistry, processing, and applications in sensors. *Chemistry of Materials*. 2015;27(16):5464-78.
55. Cacopardo L, Costa J, Giusti S, Buoncompagni L, Meucci S, Corti A, et al. Real-time cellular impedance monitoring and imaging of biological barriers in a dual-flow membrane bioreactor. *Biosensors and Bioelectronics*. 2019;140:111340.
56. Yeste J, Illa X, Gutiérrez C, Solé M, Guimerà A, Villa R. Geometric correction factor for transepithelial electrical resistance measurements in transwell and microfluidic cell cultures. *Journal of Physics D: Applied Physics*. 2016;49(37):375401.
57. Vogel PA, Halpin ST, Martin RS, Spence DM. Microfluidic transendothelial electrical resistance measurement device that enables blood flow and postgrowth experiments. *Analytical chemistry*. 2011;83(11):4296-301.
58. van der Helm MW, Odijk M, Frimat J-P, van der Meer AD, Eijkel JC, van den Berg A, et al. Direct quantification of transendothelial electrical resistance in organ-on-chips. *Biosensors and bioelectronics*. 2016;85:924-9.
59. Essig M, Friedlander G. Tubular shear stress and phenotype of renal proximal tubular cells. *Journal of the American Society of Nephrology*. 2003;14(suppl 1):S33-S5.
60. Vormann MK, Gijzen L, Hutter S, Boot L, Nicolas A, van den Heuvel A, et al. Nephrotoxicity and kidney transport assessment on 3D perfused proximal tubules. *The AAPS journal*. 2018;20(5):90.
61. Gilbert RE. Proximal Tubulopathy: Prime Mover and Key Therapeutic Target in Diabetic Kidney Disease. *Diabetes*. 2017;66(4):791-800.
62. Cabal B, Alou L, Cafini F, Couceiro R, Sevillano D, Esteban-Tejeda L, et al. A new biocompatible and antibacterial phosphate free glass-ceramic for medical applications. 2014;4:5440.
63. Moore E, Rawley O, Wood T, Galvin PJS, Chemical AB. Monitoring of cell growth in vitro using biochips packaged with indium tin oxide sensors. 2009;139(1):187-93.
64. Russo S, Ranzani T, Walsh C, Wood R, editors. A soft pop-up proprioceptive actuator for minimally invasive surgery. *The 9th Hamlyn Symposium on Medical Robotics*, London, June; 2016.
65. Hirama H, Satoh T, Sugiura S, Shin K, Onuki-Nagasaki R, Kanamori T, et al. Glass-based organ-on-a-chip device for restricting small molecular absorption. 2019;127(5):641-6.
66. Riemann A, Ihling A, Thomas J, Schneider B, Thews O, Gekle M. Acidic environment activates inflammatory programs in fibroblasts via a cAMP–MAPK pathway. *Biochimica et Biophysica ACTA (BBA)-Molecular Cell Research*. 2015;1853(2):299-307.
67. Van Eden W, Wick G, Albani S, Cohen I. Stress, heat shock proteins, and autoimmunity: how immune responses to heat shock proteins are to be used for the control of chronic inflammatory diseases. *Annals of the New York Academy of Sciences*. 2007;1113(1):217-37.
68. Barbier L, Ferhat M, Salamé E, Robin A, Herbelin A, Gombert J-M, et al. Interleukin-1 family cytokines: keystones in liver inflammatory diseases. 2019;10:2014.
69. Alegre F, Pelegrin P, Feldstein AE, editors. *Inflammasomes in liver fibrosis. Seminars in liver disease*; 2017: Thieme Medical Publishers.